



ELSEVIER

Probabilistic Engineering Mechanics 19 (2004) 393–408

PROBABILISTIC  
ENGINEERING  
MECHANICS

[www.elsevier.com/locate/probengmech](http://www.elsevier.com/locate/probengmech)

# A univariate dimension-reduction method for multi-dimensional integration in stochastic mechanics

S. Rahman\*, H. Xu

*Department of Mechanical Engineering, College of Engineering, University of Iowa, 2140 Seamans Center, Iowa City, IA 52242, USA*

Received 10 October 2003; revised 19 March 2004; accepted 29 April 2004

## Abstract

This paper presents a new, univariate dimension-reduction method for calculating statistical moments of response of mechanical systems subject to uncertainties in loads, material properties, and geometry. The method involves an additive decomposition of a multi-dimensional response function into multiple one-dimensional functions, an approximation of response moments by moments of single random variables, and a moment-based quadrature rule for numerical integration. The resultant moment equations entail evaluating  $N$  number of one-dimensional integrals, which is substantially simpler and more efficient than performing one  $N$ -dimensional integration. The proposed method neither requires the calculation of partial derivatives of response, nor the inversion of random matrices, as compared with commonly used Taylor expansion/perturbation methods and Neumann expansion methods, respectively. Nine numerical examples involving elementary mathematical functions and solid-mechanics problems illustrate the proposed method. Results indicate that the univariate dimension-reduction method provides more accurate estimates of statistical moments or multidimensional integration than first- and second-order Taylor expansion methods, the second-order polynomial chaos expansion method, the second-order Neumann expansion method, statistically equivalent solutions, the quasi-Monte Carlo simulation, and the point estimate method. While the accuracy of the univariate dimension-reduction method is comparable to that of the fourth-order Neumann expansion, a comparison of CPU time suggests that the former is computationally far more efficient than the latter.

© 2004 Elsevier Ltd. All rights reserved.

*Keywords:* Statistical moments; Multi-dimensional integration; Dimension-reduction; Stochastic mechanics; Moment-based quadrature; Stochastic finite element and meshless methods

## 1. Introduction

A common problem in computational statistics and stochastic mechanics entails calculating a multi-dimensional integral to determine the probabilistic characteristics of random output when input uncertainties are characterized either partially by moments or fully by probability density functions [1–6]. In general, such an integral cannot be evaluated analytically. Direct numerical integration can be performed, but is not economically feasible when the number of random variables increases beyond three or four. Other than numerical integration, current existing methods to solve stochastic problems can be arbitrarily classified into two

major categories: (1) classical analytical methods and (2) simulation methods.

Analytical methods include Taylor expansion or perturbation methods [7–10], the Neumann expansion method [11–15], the decomposition method [16,17], the polynomial chaos expansion method [14], the statistically equivalent solution [18], the point estimate method [19, 20], and others [1], and have been traditionally employed to predict second-moment characteristics of random output. Taylor expansion or perturbation methods involve first- or second-order Taylor series expansion of output in terms of input random parameters and application of standard stochastic operators to obtain second-moment properties of output. Two major limitations of these methods are that both the uncertainty of random input and the nonlinearity of random output with respect to random input must be small. The errors in these methods can be bounded if higher-order partial derivatives of the output

\* Corresponding author. Tel.: +1-319-335-5679; fax: +1-319-335-5669.  
E-mail address: [rahman@engineering.uiowa.edu](mailto:rahman@engineering.uiowa.edu) (S. Rahman).

variable exist and are available. However, such bounds are rarely used in engineering applications since they require expensive calculations of higher-order partial derivatives (e.g. third-order partial derivatives are needed to bound errors of second-order Taylor expansion or perturbation methods). The Neumann expansion method consists of Neumann series expansion of the inverse of random matrices (or other mathematical operators), which is absolutely convergent [1]. However, the algebra and numerical effort required for a relatively low-order Neumann expansion can be enormous when there are a large number of random variables or random fields [13–15]. The decomposition and polynomial chaos expansion methods involve alternative series expansions that can be exploited for stochastic analysis. The expansion terms in the decomposition method exhibit a recursive relationship, but the series may not be convergent [1]. The polynomial chaos expansion method is mean-square convergent and can approximate a square-integrable random variable by Hermite or chaos polynomials of Gaussian variables [3,14]. However, depending on the order of polynomial expansion, this method may provide inaccurate estimates of higher-order moments (e.g. skewness, kurtosis, etc.), as recently demonstrated by Grigoriu [1]. For problems involving large number of input variables, the number of polynomial coefficients grows exponentially and the resultant calculations become prohibitively large. Statistically equivalent solutions are based on a selection of model parameters, which can be determined from the condition that the difference between exact and approximate responses is in some sense minimized. However, this difference cannot be calculated directly since the exact probability law of output is unknown. The point estimate method involves finite number of probability concentrations to approximate second-moment properties of response. Similar to Taylor expansion methods, the point estimate method also yields inaccurate results when input uncertainties are moderate to large [19]. In summary, all existing methods described above become computationally inefficient or less accurate when the number or the uncertainty of input random variables is large. Hence, new stochastic methods, which are derivative-free and can handle arbitrarily large number of random variables, and yet predict both response moments and reliability accurately, are highly desirable.

Simulation methods involving sampling and estimation are well known in the statistics and reliability literature. Direct Monte Carlo simulation [21] is the most widely used simulation method and involves the generation of independent samples of all input random variables, repeated deterministic trials (analyses) to obtain corresponding simulated samples of response variables, and standard statistical analysis to estimate probabilistic characteristics of response. This method generally requires a large number of simulations to calculate low probability or higher-order moments, and is impractical

when each simulation involves expensive finite-element or meshless calculations. As a result, researchers have developed or examined faster simulation methods, such as quasi-Monte Carlo simulation [22–24], importance sampling [25,26], directional simulation [27,28], and others [29–32]. Nevertheless, all simulation methods today require considerably more extensive calculations than analytical methods. Consequently, simulation methods have found their utility when alternative methods are inapplicable or inaccurate, and/or analytical methods require validation.

This paper presents a new dimension-reduction method for predicting second-moment characteristics of response of mechanical systems subject to random loads, material properties, and geometry. The method involves an additive decomposition of a multi-dimensional response function into multiple one-dimensional functions; an approximation of response moments by moments of single random variables; and a moment-based quadrature rule for numerical integration. Two sets of numerical examples illustrate the accuracy and/or computational efficiency of the proposed method.

## 2. Univariate dimension-reduction method

### 2.1. Additive decomposition and reduced integration

Consider a continuous, differentiable, real-valued function  $y(x_1, x_2)$  that depends on two independent variables  $x_1 \in \mathfrak{R}$  and  $x_2 \in \mathfrak{R}$ . Let

$$I[y(x_1, x_2)] \equiv \int_{-a}^{+a} \int_{-a}^{+a} y(x_1, x_2) dx_1 dx_2, \quad (1)$$

denote a two-dimensional integration of  $y(x_1, x_2)$  on the symmetric range  $[-a, a]^2$ . If the Taylor series expansion of  $y(x_1, x_2)$  at  $(x_1 = 0, x_2 = 0)$ , expressed by

$$\begin{aligned} y(x_1, x_2) = & y(0, 0) + \frac{\partial y}{\partial x_1}(0, 0)x_1 + \frac{\partial y}{\partial x_2}(0, 0)x_2 \\ & + \frac{1}{2!} \frac{\partial^2 y}{\partial x_1^2}(0, 0)x_1^2 + \frac{1}{2!} \frac{\partial^2 y}{\partial x_2^2}(0, 0)x_2^2 \\ & + \frac{\partial^2 y}{\partial x_1 \partial x_2}(0, 0)x_1 x_2 + \frac{1}{3!} \frac{\partial^3 y}{\partial x_1^3}(0, 0)x_1^3 \\ & + \frac{1}{3!} \frac{\partial^3 y}{\partial x_2^3}(0, 0)x_2^3 + \frac{1}{2!} \frac{\partial^3 y}{\partial x_1^2 \partial x_2}(0, 0)x_1^2 x_2 \\ & + \frac{1}{2!} \frac{\partial^3 y}{\partial x_1 \partial x_2^2}(0, 0)x_1 x_2^2 + \frac{1}{4!} \frac{\partial^4 y}{\partial x_1^4}(0, 0)x_1^4 \\ & + \frac{1}{4!} \frac{\partial^4 y}{\partial x_2^4}(0, 0)x_2^4 + \frac{1}{3!} \frac{\partial^4 y}{\partial x_1^3 \partial x_2}(0, 0)x_1^3 x_2 \\ & + \frac{1}{2!} \frac{\partial^4 y}{\partial x_1^2 \partial x_2^2}(0, 0)x_1^2 x_2^2 + \frac{1}{3!} \frac{\partial^4 y}{\partial x_1 \partial x_2^3}(0, 0)x_1 x_2^3 \\ & + \dots \end{aligned} \quad (2)$$

is convergent and substituted in Eq. (1), the integral becomes

$$\begin{aligned}
 I[y(x_1, x_2)] &= I[y(0, 0)] + \frac{1}{2!} \frac{\partial^2 y}{\partial x_1^2}(0, 0)I[x_1^2] \\
 &+ \frac{1}{2!} \frac{\partial^2 y}{\partial x_2^2}(0, 0)I[x_2^2] + \frac{1}{4!} \frac{\partial^4 y}{\partial x_1^4}(0, 0)I[x_1^4] \\
 &+ \frac{1}{4!} \frac{\partial^4 y}{\partial x_2^4}(0, 0)I[x_2^4] \\
 &+ \frac{1}{2!2!} \frac{\partial^4 y}{\partial x_1^2 \partial x_2^2}(0, 0)I[x_1^2 x_2^2] + \dots, \quad (3)
 \end{aligned}$$

where terms

$$\begin{aligned}
 I[x_1^{k_1} x_2^{k_2}] &= \int_{-a}^{+a} \int_{-a}^{+a} x_1^{k_1} x_2^{k_2} dx_1 dx_2 = \int_{-a}^{+a} x_2^{k_2} dx_2 \\
 &\times \int_{-a}^{+a} x_1^{k_1} dx_1 = 0,
 \end{aligned}$$

when  $k_1$  or  $k_2$  is an odd integer. Now consider an additive decomposition

$$\hat{y}(x_1, x_2) = y(x_1, 0) + y(0, x_2) - y(0, 0), \quad (4)$$

where each of the first two terms on the right-hand side is a function of only one variable and can be subsequently expanded in Taylor series at  $(x_1 = 0, x_2 = 0)$ , yielding

$$\begin{aligned}
 \hat{y}(x_1, x_2) &= y(0, 0) + \frac{\partial y}{\partial x_1}(0, 0)x_1 + \frac{\partial y}{\partial x_2}(0, 0)x_2 \\
 &+ \frac{1}{2!} \frac{\partial^2 y}{\partial x_1^2}(0, 0)x_1^2 + \frac{1}{2!} \frac{\partial^2 y}{\partial x_2^2}(0, 0)x_2^2 \\
 &+ \frac{1}{3!} \frac{\partial^3 y}{\partial x_1^3}(0, 0)x_1^3 + \frac{1}{3!} \frac{\partial^3 y}{\partial x_2^3}(0, 0)x_2^3 \\
 &+ \frac{1}{4!} \frac{\partial^4 y}{\partial x_1^4}(0, 0)x_1^4 + \frac{1}{4!} \frac{\partial^4 y}{\partial x_2^4}(0, 0)x_2^4 + \dots \quad (5)
 \end{aligned}$$

The comparison of Eqs. (2) and (5) indicates that  $y(x_1, x_2)$  contains all terms of  $\hat{y}(x_1, x_2)$ , and it is interesting to note that

$$\begin{aligned}
 I[\hat{y}(x_1, x_2)] &= I[y(0, 0)] + \frac{1}{2!} \frac{\partial^2 y}{\partial x_1^2}(0, 0)I[x_1^2] \\
 &+ \frac{1}{2!} \frac{\partial^2 y}{\partial x_2^2}(0, 0)I[x_2^2] + \frac{1}{4!} \frac{\partial^4 y}{\partial x_1^4}(0, 0)I[x_1^4] \\
 &+ \frac{1}{4!} \frac{\partial^4 y}{\partial x_2^4}(0, 0)I[x_2^4] + \dots \quad (6)
 \end{aligned}$$

provides a univariate approximation of  $I[y(x_1, x_2)]$  by including all one-dimensional integrations in Eq. (3), with the residual error

$$\begin{aligned}
 I[y(x_1, x_2)] - I[\hat{y}(x_1, x_2)] \\
 = \frac{1}{2!2!} \frac{\partial^4 y}{\partial x_1^2 \partial x_2^2}(0, 0)I[x_1^2 x_2^2] + \dots \quad (7)
 \end{aligned}$$

For a generalization to  $N$  number of variables, consider a continuous, differentiable, real-valued function  $y(\mathbf{x})$  that depends on  $\mathbf{x} = \{x_1, \dots, x_N\} \in \mathfrak{R}^N$ . If

$$I[y(\mathbf{x})] \equiv \int_{-a}^{+a} \dots \int_{-a}^{+a} y(x_1, \dots, x_N) dx_1 \dots dx_N \quad (8)$$

defines an  $N$ -dimensional integration of  $y(\mathbf{x})$  in the range  $[-a, a]^N$ , then by following Taylor series expansion of  $y(\mathbf{x})$  at  $\mathbf{x} = \mathbf{0} = \{0, \dots, 0\}^T$ , it can be expressed by

$$\begin{aligned}
 I[y(\mathbf{x})] &= I[y(\mathbf{0})] + \frac{1}{2!} \sum_{i=1}^N \frac{\partial^2 y}{\partial x_i^2}(\mathbf{0})I[x_i^2] + \frac{1}{4!} \sum_{i=1}^N \frac{\partial^4 y}{\partial x_i^4}(\mathbf{0})I[x_i^4] \\
 &+ \frac{1}{2!2!} \sum_{i < j} \frac{\partial^4 y}{\partial x_i^2 \partial x_j^2}(\mathbf{0})I[x_i^2 x_j^2] + \dots, \quad (9)
 \end{aligned}$$

where once again the terms  $I[\prod_{i=1}^N x_i^{k_i}]$  vanish when  $k_i$  is an odd integer for some  $i$ . Analogous to Eq. (4), consider a univariate approximation

$$\begin{aligned}
 \hat{y}(\mathbf{x}) &\equiv \hat{y}(x_1, \dots, x_N) \\
 &= \sum_{i=1}^N y(0, \dots, 0, x_i, 0, \dots, 0) - (N-1)y(0, \dots, 0), \quad (10)
 \end{aligned}$$

where each term in the summation is a function of only one variable and can be subsequently expanded in a Taylor series at  $\mathbf{x} = \mathbf{0}$ , yielding

$$\begin{aligned}
 I[\hat{y}(\mathbf{x})] &= I[y(\mathbf{0})] + \frac{1}{2!} \sum_{i=1}^N \frac{\partial^2 y}{\partial x_i^2}(\mathbf{0})I[x_i^2] \\
 &+ \frac{1}{4!} \sum_{i=1}^N \frac{\partial^4 y}{\partial x_i^4}(\mathbf{0})I[x_i^4] + \dots \quad (11)
 \end{aligned}$$

Similar to Eq. (7), the univariate approximation leads to the residual error

$$I[y(\mathbf{x})] - I[\hat{y}(\mathbf{x})] = \frac{1}{2!2!} \sum_{i < j} \frac{\partial^4 y}{\partial x_i^2 \partial x_j^2}(\mathbf{0})I[x_i^2 x_j^2] + \dots, \quad (12)$$

which includes contributions from integrations of dimension two and higher. For sufficiently smooth  $y(\mathbf{x})$  with convergent Taylor series, the coefficients [e.g.  $(1/2!2!)\partial^4 y(\mathbf{0})/\partial x_i^2 \partial x_j^2$ ] associated with higher-dimensional integrations are much smaller than that with one-dimensional integrations. In that case, terms associated with higher-dimensional integrations can be neglected. In contrast, the residual error due to the second-order Taylor approximation  $\tilde{y}_2(\mathbf{x})$ , given by

$$\begin{aligned}
 I[y(\mathbf{x})] - I[\tilde{y}_2(\mathbf{x})] &= \frac{1}{4!} \sum_{i=1}^N \frac{\partial^4 y}{\partial x_i^4}(\mathbf{0})I[x_i^4] \\
 &+ \frac{1}{2!2!} \sum_{i < j} \frac{\partial^4 y}{\partial x_i^2 \partial x_j^2}(\mathbf{0})I[x_i^2 x_j^2] + \dots, \quad (13)
 \end{aligned}$$

comprises one- (fourth order and higher), two-, and higher-dimensional integrations. In either case, contributions from bivariate and higher-dimensional integrations are retained

in the residual errors. This issue is addressed in Section 3.1. Note that  $I[\hat{y}(\mathbf{x})]$  represents a reduced integration, because only  $N$  number of one-dimensional integration is required, as opposed to one  $N$ -dimensional integration in  $I[y(\mathbf{x})]$ . Furthermore, there is no need to calculate partial derivatives. If, indeed, the contributions from two- and higher-dimensional integrations are negligibly small, then  $I[\hat{y}(\mathbf{x})]$  in Eq. (11) provides a convenient approximation of  $I[y(\mathbf{x})]$ . Furthermore, Eq. (11) yields exact results when  $y(\mathbf{x}) = \sum_{i=1}^N y_i(x_i)$ , i.e. when  $y(\mathbf{x})$  can be additively decomposed into functions  $y_i(x_i)$  of single variables.

2.2. Non-symmetric domains and arbitrary expansion point

In order to integrate over a non-symmetric domain  $\prod_{i=1}^N [a_i, b_i]$ , such as

$$I[y(\mathbf{x})] = \int_{a_N}^{b_N} \cdots \int_{a_1}^{b_1} y(x_1, \dots, x_N) dx_1 \cdots dx_N, \tag{14}$$

a linear transformation

$$x_i = \frac{b_i + a_i}{2} + \frac{b_i - a_i}{2} \xi_i, \quad i = 1, \dots, N \tag{15}$$

maps the original integral over a non-symmetric domain, to

$$I[y(\mathbf{x})] = \prod_{i=1}^N \frac{b_i - a_i}{2} \int_{-1}^1 \cdots \int_{-1}^1 \eta(\xi_1, \dots, \xi_N) d\xi_1 \cdots d\xi_N, \tag{16}$$

which represents an integral over a symmetric domain where  $\eta(\xi_1, \dots, \xi_N)$  is the transformed function due to a change of variables from  $\mathbf{x}$  to  $\boldsymbol{\xi}$ -space. Hence, Eq. (12) is applicable to a multi-dimensional integration over non-symmetric domains.

Eq. (10) is developed based on the additive decomposition centered at  $\mathbf{x} = \mathbf{0}$ . For any arbitrary point  $\mathbf{x} = \boldsymbol{\mu}$ , a slightly generalized form of Eq. (10) can be given as

$$\hat{y}(\mathbf{x}) = \hat{y}(x_1, \dots, x_N) \equiv \sum_{i=1}^N y(\boldsymbol{\mu}_1, \dots, \boldsymbol{\mu}_{i-1}, x_i, \boldsymbol{\mu}_{i+1}, \dots, \boldsymbol{\mu}_N) - (N - 1)y(\boldsymbol{\mu}_1, \dots, \boldsymbol{\mu}_N), \tag{17}$$

yielding the reduced integration

$$I[\hat{y}(\mathbf{x})] = \sum_{i=1}^N I[y(\boldsymbol{\mu}_1, \dots, \boldsymbol{\mu}_{i-1}, x_i, \boldsymbol{\mu}_{i+1}, \dots, \boldsymbol{\mu}_N)] - (N - 1)I[y(\boldsymbol{\mu}_1, \dots, \boldsymbol{\mu}_N)]. \tag{18}$$

Eqs. (17) and (18) will be employed for solving stochastic problems, as follows.

3. Application to stochastic problems

3.1. Statistical moments of response

Consider a mechanical system subject to random input vector  $\mathbf{X} = \{X_1, \dots, X_N\}^T \in \mathfrak{R}^N$ , which characterizes

uncertainty in loads, material properties, and geometry. Let  $Y(\mathbf{X})$  represent a relevant response of interest, for which its  $l$ th statistical moment

$$m_l \equiv \mathcal{E}[Y^l(\mathbf{X})] = \int_{\mathfrak{R}^N} y^l(\mathbf{x}) f_{\mathbf{X}}(\mathbf{x}) d\mathbf{x} \tag{19}$$

is sought, where  $f_{\mathbf{X}}(\mathbf{x}) = f_{X_1, \dots, X_N}(x_1, \dots, x_N)$  is the joint probability density function of  $\mathbf{X}$  and  $\mathcal{E}$  is the expectation operator. Following the dimension-reduction procedure in Eqs. (17) and (18), the  $l$ th moment can be approximated by

$$m_l \cong \mathcal{E}[\hat{Y}^l(\mathbf{X})] = \mathcal{E} \left[ \left\{ \sum_{j=1}^N Y(\boldsymbol{\mu}_1, \dots, \boldsymbol{\mu}_{j-1}, X_j, \boldsymbol{\mu}_{j+1}, \dots, \boldsymbol{\mu}_N) - (N - 1)y(\boldsymbol{\mu}_1, \dots, \boldsymbol{\mu}_N) \right\}^l \right], \tag{20}$$

where  $\boldsymbol{\mu}_j \equiv \mathcal{E}[X_j]$  is the first moment or mean of  $X_j$ ,  $Y(\boldsymbol{\mu}_1, \dots, \boldsymbol{\mu}_{j-1}, X_j, \boldsymbol{\mu}_{j+1}, \dots, \boldsymbol{\mu}_N)$  is a random response that depends on the  $j$ th random variable  $X_j$ ,  $y(\boldsymbol{\mu}_1, \dots, \boldsymbol{\mu}_N)$  is a deterministic response when  $\{X_1 = \boldsymbol{\mu}_1, \dots, X_N = \boldsymbol{\mu}_N\}$ . Applying the binomial formula on the right-hand side of Eq. (20) gives

$$m_l \cong \sum_{i=0}^l \binom{l}{i} \mathcal{E} \left\{ \sum_{j=1}^N Y(\boldsymbol{\mu}_1, \dots, \boldsymbol{\mu}_{j-1}, X_j, \boldsymbol{\mu}_{j+1}, \dots, \boldsymbol{\mu}_N) \right\}^i [- (N - 1)y(\boldsymbol{\mu}_1, \dots, \boldsymbol{\mu}_N)]^{l-i}. \tag{21}$$

Define

$$S_j^i = \mathcal{E} \left[ \left\{ \sum_{i=1}^j Y(\boldsymbol{\mu}_1, \dots, \boldsymbol{\mu}_{i-1}, X_i, \boldsymbol{\mu}_{i+1}, \dots, \boldsymbol{\mu}_N) \right\}^i \right]; \tag{22}$$

$j = 1, \dots, N; i = 1, \dots, l$ ,

which can be expressed using the recursive formula

$$S_1^i = \mathcal{E}[Y^i(X_1, \boldsymbol{\mu}_2, \dots, \boldsymbol{\mu}_N)]; \quad i = 1, \dots, l$$

$$S_2^i = \sum_{k=0}^i \binom{i}{k} S_1^k \mathcal{E}[Y^{i-k}(\boldsymbol{\mu}_1, X_2, \boldsymbol{\mu}_3, \dots, \boldsymbol{\mu}_N)]; \quad i = 1, \dots, l$$

$$S_3^i = \sum_{k=0}^i \binom{i}{k} S_2^k \mathcal{E}[Y^{i-k}(\boldsymbol{\mu}_1, \boldsymbol{\mu}_2, X_3, \boldsymbol{\mu}_4, \dots, \boldsymbol{\mu}_N)]; \quad i = 1, \dots, l$$

⋮

$$S_j^i = \sum_{k=0}^i \binom{i}{k} S_{j-1}^k \mathcal{E}[Y^{i-k}(\boldsymbol{\mu}_1, \dots, \boldsymbol{\mu}_{j-1}, X_j, \boldsymbol{\mu}_{j+1}, \dots, \boldsymbol{\mu}_N)]; \quad i = 1, \dots, l$$

⋮

$$S_N^i = \sum_{k=0}^i \binom{i}{k} S_{N-1}^k \mathcal{E}[Y^{i-k}(\boldsymbol{\mu}_1, \dots, \boldsymbol{\mu}_{N-1}, X_N)]; \quad i = 1, \dots, l. \tag{23}$$

Hence, Eq. (21) becomes

$$m_l \cong \mathcal{E}[\hat{Y}^l(\mathbf{X})] = \sum_{i=0}^l \binom{l}{i} S_N^i [- (N-1) y(\mu_1, \dots, \mu_N)]^{l-i}. \quad (24)$$

In Eqs. (23) and (24), one needs to compute  $\mathcal{E}[Y^m(\mu_1, \dots, \mu_{j-1}, X_j, \mu_{j+1}, \dots, \mu_N)]$ ;  $m = i - k$ . According to the definition,

$$\mathcal{E}[Y^m(\mu_1, \dots, \mu_{j-1}, X_j, \mu_{j+1}, \dots, \mu_N)] = \int_{-\infty}^{\infty} y^m(\mu_1, \dots, \mu_{j-1}, x_j, \mu_{j+1}, \dots, \mu_N) f_{X_j}(x_j) dx_j, \quad (25)$$

where  $f_{X_j}(x_j)$  is the marginal probability density of  $X_j$ , which can be calculated from the known joint density of  $\mathbf{X}$ .

Note that Eq. (25) is valid for independent random vector  $\mathbf{X}$ . However, if  $\mathbf{X}$  comprises dependent variables with its joint density  $f_{\mathbf{X}}(\mathbf{x}) = f_{X_1, \dots, X_N}(x_1, \dots, x_N)$ , a multivariate transformation such as Rosenblatt transformation [33] should be applied to transform the dependent random vector  $\mathbf{X}$  to an independent standard Gaussian random vector  $\mathbf{U}$ . The Rosenblatt transformation is given by [33]

$$\begin{aligned} u_1 &= \Phi^{-1}[F_{X_1}(x_1)] \\ u_2 &= \Phi^{-1}[F_{X_2}(x_2|x_1)] \\ &\vdots \\ u_N &= \Phi^{-1}[F_{X_N}(x_N|x_1, x_2, \dots, x_{N-1})], \end{aligned} \quad (26)$$

in which  $F_{X_i}(x_i|x_1, x_2, \dots, x_{i-1})$  is the cumulative distribution function of component  $X_i$  conditional on  $X_1 = x_1, X_2 = x_2, \dots, X_{i-1} = x_{i-1}$  and  $\Phi(\cdot)$  is the cumulative distribution function of a standard Gaussian random variable. The conditional distribution function  $F_{X_i}(x_i|x_1, x_2, \dots, x_{i-1})$  can be obtained from

$$F_{X_i}(x_i|x_1, x_2, \dots, x_{i-1}) = \frac{\int_{-\infty}^{x_i} f_{X_1, X_2, \dots, X_i}(x_1, x_2, \dots, x_{i-1}, s) ds}{f_{X_1, X_2, \dots, X_{i-1}}(x_1, x_2, \dots, x_{i-1})}, \quad (27)$$

where  $f_{X_1, X_2, \dots, X_{i-1}}(x_1, x_2, \dots, x_{i-1})$  is the joint probability density function of random vector  $\{X_1, X_2, \dots, X_{i-1}\}^T$ . Notice that Eq. (25) only require one-dimensional deterministic integration that can easily be evaluated using standard quadrature rules. For example, Gauss–Legendre and Gauss–Hermite quadratures are frequently used when  $X_j$  follows uniform and Gaussian probability distributions, respectively [34]. For arbitrary distribution of  $X_j$ , a moment-based quadrature rule, described in the subsequent section, was developed to evaluate the integral.

The newly proposed moment equation entails evaluating  $N$  number of one-dimensional integrals, which is substantially simpler and more efficient than performing one  $N$ -dimensional integration. For practical problems involving a moderate to large number of random variables (e.g.  $N > 10$ ), this is a promising method. The method does not require calculation of any partial derivatives of response or inversion of random matrices when compared with the commonly used Taylor/perturbation and Neumann expansion methods, respectively. Hence, the computation effort in conducting probabilistic finite element or meshless analysis will be significantly reduced by the dimension-reduction method. The method is coined *univariate dimension-reduction*, because it essentially reduces the calculation of an  $N$ -dimensional integral to that of a one-dimensional integral. It is also noted that when  $N = 1$ , the integrand becomes a univariate function, i.e., no dimension reduction is possible or required and the proposed method is exact.

As described previously, the residual error in the univariate dimension-reduction method contains terms involving bivariate and other higher-dimensional integrations. The error can be reduced further, for example, in the bivariate reduction method, if terms associated with bivariate integrations are retained in  $\hat{y}(\mathbf{x})$ . However, this process will require two-dimensional integrations, as opposed to one-dimensional integrations in the univariate dimension-reduction method. Nevertheless, it is conceivable that bivariate and, in general, multivariate dimension-reduction methods can be developed to reduce residual error to an arbitrarily small number, which is a subject of current research by the authors.

### 3.2. Moment-based quadrature rule

In this section, a new moment-consistent quadrature rule is presented to perform numerical integration in the direction of the  $x_j$  coordinate, as defined in Eq. (25). To construct a moment-consistent integration rule with  $n$  interpolation points  $x_{j,i}, i = 1, \dots, n$  in the direction of the  $x_j$  co-ordinate, define a function

$$P(x_j) = \prod_{i=1}^n (x_j - x_{j,i}) f_{X_j}(x_j), \quad (28)$$

which satisfies

$$\int_{-\infty}^{\infty} P(x_j)(x_j)^i dx_j = 0; \quad i = 0, 1, \dots, n - 1. \quad (29)$$

If

$$r_{j,k} = \sum_{i_1=1}^n \sum_{i_2=1, \neq i_1}^n \dots \sum_{i_k=1, \neq i_1, i_2, \dots, i_{k-1}}^n x_{j,i_1} x_{j,i_2} \dots x_{j,i_k}; \quad (30)$$

$k = 1, 2, \dots, n,$

Eq. (29) yields a system of linear equations

$$\begin{bmatrix} \mu_{j,n-1} & -\mu_{j,n-2} & \mu_{j,n-3} & \cdots & (-1)^{n-1} \mu_{j,0} \\ \mu_{j,n} & -\mu_{j,n-1} & \mu_{j,n-2} & \cdots & (-1)^{n-1} \mu_{j,1} \\ \mu_{j,n+1} & -\mu_{j,n} & \mu_{j,n-1} & \cdots & (-1)^{n-1} \mu_{j,2} \\ \vdots & \vdots & \vdots & \vdots & \vdots \\ \mu_{j,2n-2} & -\mu_{j,2n-3} & \mu_{j,2n-4} & \cdots & (-1)^{n-1} \mu_{j,n-1} \end{bmatrix} \begin{bmatrix} r_{j,1} \\ r_{j,2} \\ r_{j,3} \\ \vdots \\ r_{j,n} \end{bmatrix} = \begin{bmatrix} \mu_{j,n} \\ \mu_{j,n+1} \\ \mu_{j,n+2} \\ \vdots \\ \mu_{j,2n-1} \end{bmatrix}, \quad (31)$$

where the coefficient matrix consists of known moments of input random variable  $X_j$ , given by

$$\mu_{j,i} = \int_{-\infty}^{\infty} (x_j)^i f_{X_j}(x_j) dx_j. \quad (32)$$

After solving  $r_{j,i}$  from Eq. (31), the interpolation point  $x_{j,i}$ ,  $i = 1, \dots, n$  can easily be obtained as the  $i$ th root of

$$x_j^n - r_{j,1} x_j^{n-1} + r_{j,2} x_j^{n-2} - \dots + (-1)^n r_{j,n} = 0. \quad (33)$$

For a shape function defined as

$$\phi_{j,i}^{(n-1)}(x_j) \equiv \frac{f_{X_j}(x_j) \prod_{k=1, k \neq i}^n (x_j - x_{j,k})}{f_{X_j}(x_{j,i}) \prod_{k=1, k \neq i}^n (x_{j,i} - x_{j,k})}, \quad (34)$$

it can be shown by polynomial approximation that

$$\begin{aligned} & y^m(\mu_1, \dots, \mu_{j-1}, x_j, \mu_{j+1}, \dots, \mu_N) f_{X_j}(x_j) \\ & \cong \sum_{i=1}^n \phi_{j,i}^{(n-1)}(x_j) y^m(\mu_1, \dots, \mu_{j-1}, x_{j,i}, \mu_{j+1}, \dots, \mu_N) \\ & \quad \times f_{X_j}(x_{j,i}) + \sum_{i=0}^{n-1} \beta_{j,i}(x_j)^i P(x_j), \end{aligned} \quad (35)$$

where  $\beta_{j,i} \in (-\infty, \infty)$ ,  $i = 0, n - 1$  are constants. Hence, Eqs. (29) and (35) yield

$$\begin{aligned} & \mathcal{E}[Y^m(\mu_1, \dots, \mu_{j-1}, X_j, \mu_{j+1}, \dots, \mu_N)] \\ & \cong \sum_{i=1}^n w_{j,i} y^m(\mu_1, \dots, \mu_{j-1}, x_{j,i}, \mu_{j+1}, \dots, \mu_N), \end{aligned} \quad (36)$$

where

$$w_{j,i} = \frac{\int_{-\infty}^{\infty} \prod_{k=1, k \neq i}^n (x_j - x_{j,k}) f_{X_j}(x_j) dx_j}{\prod_{k=1, k \neq i}^n (x_{j,i} - x_{j,k})} = \frac{\sum_{k=0}^{n-1} (-1)^k \mu_{j,n-k-1} q_{j,ik}}{\prod_{k=1, k \neq i}^n (x_{j,i} - x_{j,k})} \quad (37)$$

is the  $i$ th weight for the  $j$ th variable  $X_j$ , which is consistent with its moments,  $q_{j,i0} = 1$ , and  $q_{j,ik} = r_{j,k} - x_{j,i} q_{j,i(k-1)}$ . For  $n$ -order interpolation, Eq. (37) is employed to calculate weights, and then Eq. (36) is invoked to calculate  $\mathcal{E}[Y^m(\mu_1, \dots, \mu_{j-1}, X_j, \mu_{j+1}, \dots, \mu_N)]$ . Note that the interpolation points (Eq. (33)) and the weights (Eq. (37)) are strictly based on moments of input random variables. Only a finite number of input moments are needed to calculate the output moments. The input moments can easily be obtained from its known probability distribution, or they can be estimated from its samples. Also, it can be shown that Eq. (33) generates integration points and Eq. (37) produces the weights of Gauss–Legendre or Gauss–Hermite quadratures [34] when the input random variable follows uniform or Gaussian probability distributions, respectively.

### 3.3. Discrete equilibrium equations

Consider a linear mechanical system subject to a vector of input random parameters  $X \in \mathfrak{R}^N \mapsto (\boldsymbol{\mu}, \boldsymbol{\gamma})$  characterizing uncertainty in the system and loads. Following discretization, let  $Y \in \mathfrak{R}^M \mapsto (\boldsymbol{m}_Y, \boldsymbol{\gamma}_Y)$  represent a displacement (response) vector associated with  $M$  degrees of freedom of the system, satisfying the linear equilibrium equation

$$\mathbf{K}(X)\mathbf{Y}(X) = \mathbf{F}(X), \quad (38)$$

in which stiffness matrix  $\mathbf{K}$  and force vector  $\mathbf{F}$  depend on  $X$  and represent an elementary stochastic linear operator that has random coefficients and only involves algebraic operations. Eq. (38) is common to finite-difference, finite-element, and recently developed mesh-free methods when the system, loads, or both, are uncertain. From Eq. (38), the solution

$$\mathbf{Y}(X) = \mathbf{K}(X)^{-1} \mathbf{F}(X) \quad (39)$$

is random and depends on  $X$ . Using the dimension-reduction method, the mean vector  $\boldsymbol{m}_Y$  and covariance matrix  $\boldsymbol{\gamma}_Y$  of  $Y$  can be derived as

$$\boldsymbol{m}_Y = \mathcal{E}[\mathbf{Y}] = \sum_{j=1}^N \mathcal{E}[\mathbf{K}_j(X_j)^{-1} \mathbf{F}_j(X_j)] - (N - 1) \mathbf{K}(\boldsymbol{\mu})^{-1} \mathbf{F}(\boldsymbol{\mu}) \quad (40)$$

$$\boldsymbol{\gamma}_Y = \mathcal{E}[\mathbf{Y}\mathbf{Y}^T] - \boldsymbol{m}_Y \boldsymbol{m}_Y^T \quad (41)$$

$$\mathcal{E}[\mathbf{Y}\mathbf{Y}^T] = \sum_{j=1}^N \mathcal{E}[\mathbf{K}_j(X_j)^{-1} \mathbf{F}_j(X_j) \mathbf{F}_j(X_j)^T \mathbf{K}_j(X_j)^{-T}] - (N-1) \mathbf{K}(\boldsymbol{\mu})^{-1} \mathbf{F}(\boldsymbol{\mu}) \mathbf{F}(\boldsymbol{\mu})^T \mathbf{K}(\boldsymbol{\mu})^{-T}, \quad (42)$$

where  $\mathbf{K}(\boldsymbol{\mu}) = \mathbf{K}(\mu_1, \dots, \mu_N)$ ,  $\mathbf{F}(\boldsymbol{\mu}) = \mathbf{F}(\mu_1, \dots, \mu_N)$ ,  $\mathbf{K}_j(X_j) = \mathbf{K}(\mu_1, \dots, \mu_{j-1}, X_j, \mu_{j+1}, \dots, \mu_N)$ , and  $\mathbf{F}_j(X_j) = \mathbf{F}(\mu_1, \dots, \mu_{j-1}, X_j, \mu_{j+1}, \dots, \mu_N)$ . Note that the calculation of expected values on the right-hand side of Eqs. (40) and (42) involves only one-dimensional integrations.

### 4. Numerical examples

In this section, two sets of numerical examples, one involving elementary mathematical functions (Examples 1–5) and the other involving solid-mechanics problems (Examples 6–9), are presented to illustrate the proposed univariate dimension-reduction method. For all these examples, the response functions are smooth and have convergent Taylor series at the expansion point. In these examples, the number ( $n$ ) of interpolation points in the dimension-reduction method varies from 3 to 4. Whenever possible, comparisons have been made with alternative analytical and simulation methods and direct numerical integration to evaluate the accuracy and computational efficiency of the proposed method.

#### 4.1. Example Set I: mathematical functions

**Example 1.** Consider two elementary transformations

$$Y_1 = Y_1(X_1, X_2) = \frac{1}{1 + X_1^4 + 2X_2^2 + 5X_2^4} \quad (43)$$

and

$$Y_2 = Y_2(X_1, X_2) = \exp\left(-\frac{1}{1 + 100X_1^2 + 2X_2^2 + X_1^2X_2^2}\right), \quad (44)$$

where  $X_j \mapsto N(0, \sigma^2)$ ,  $j = 1, 2$  are two independent and identically distributed Gaussian random variables with mean zero and variance  $\sigma^2$ . The proposed univariate dimension-reduction method was employed to determine standard deviations  $\sigma_{Y_1}$  and  $\sigma_{Y_2}$  of  $Y_1$  and  $Y_2$ , respectively, and are plotted in Fig. 1(a) and (b) for increasing values of input standard deviation. The dimension-reduction method provides very good approximations of  $\sigma_{Y_1}$  and  $\sigma_{Y_2}$ , when compared with the results of direct numerical integration (the reference solution). Since this problem only has two dimensions, the computational effort using the dimension-reduction method is slightly lower than with numerical integration. Comparison with the second-order Taylor expansion, the results of which are also shown in Fig. 1(a) and (b), suggests that the univariate

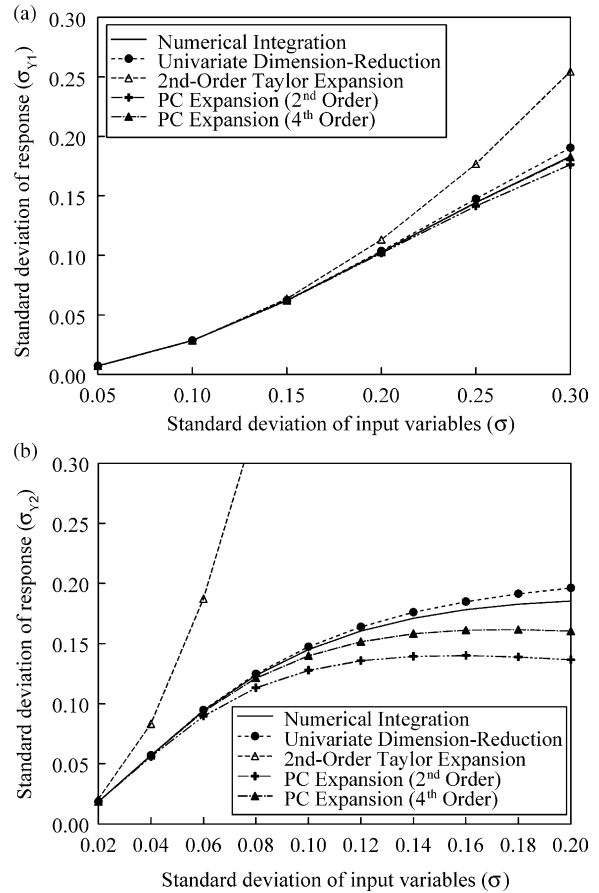


Fig. 1. Standard deviations of output responses for increasing values of input standard deviation; (a)  $Y_1 = (1 + X_1^4 + 2X_2^2 + 5X_2^4)^{-1}$ ; (b)  $Y_2 = \exp[-(1 + 100X_1^2 + 2X_2^2 + X_1^2X_2^2)^{-1}]$ .

dimension-reduction method is superior to the second-order Taylor expansion when the standard deviation of input (Fig. 1(a)) or output nonlinearity (Fig. 1(b)) is large in this particular problem. Also plotted in Fig. 1(a) and (b) are the results by second- and fourth-order polynomial chaos expansions with Hermite polynomials [14]. For both cases, the univariate dimension-reduction method is more accurate than the second-order polynomial chaos expansion. For case (a), Fig. 1(a) indicates that the fourth-order polynomial chaos expansion can generate more accurate result than the univariate dimension-reduction method. However, CPU time associated with the calculation of 14 coefficients in the fourth-order polynomial chaos expansion makes it more expensive than the univariate dimension-reduction method.

**Example 2.** Consider a stochastic response function

$$Y = Y(X_1, X_2, X_3) = 3X_1^2 - X_1X_2 + X_1X_3 + X_3^3, \quad (45)$$

where  $X_j \in [0, \infty)$ ,  $j = 1, 2, 3$  are three independent and identically distributed Weibull random variables with mean 0.918 and standard deviation 0.210, and marginal

Table 1  
Statistical moments of  $Y$  by Taylor expansion and dimension-reduction methods

Statistical moments of $Y(m_l = \mathcal{E}[Y^l])$	First-order Taylor expansion method	Second-order Taylor expansion method	Univariate dimension-reduction method	Numerical integration
$m_1$	3.3032	3.5577	3.5553	3.5553
$m_2$	12.816	14.504	14.519	14.523

probability density function  $f_{X_j}(x_j) = 5x_j^4 \exp(-x_j^5)$ . Table 1 shows the first and second moments of response

$$m_l \equiv \mathcal{E}[Y^l(X_1, X_2, X_3)] = \int_{\mathbb{R}^3} y^l(x_1, x_2, x_3) \prod_{j=1}^3 f_{X_j}(x_j) dx_j; \quad l = 1, 2 \quad (46)$$

obtained using the univariate dimension-reduction method, first- and second-order Taylor expansion methods, and direct numerical integration. Results show that the dimension-reduction method provides more accurate estimates of response moments than either the first- or second-order Taylor expansion methods, which is similar to the conclusion reached for Example 1.

**Example 3.** This example illustrates how the dimension affects the calculation of a multi-dimensional integral. Define  $y(x_1, \dots, x_N) = \prod_{i=1}^N \sin(\pi x_i)$ , for which a multi-dimensional integral, given by

$$I[y(x_1, \dots, x_N)] \equiv \int_0^2 \cdots \int_0^2 y(x_1, \dots, x_N) \prod_{i=1}^N dx_i, \quad (47)$$

is sought. The integral in Eq. (47) was calculated using the univariate dimension-reduction method and Monte Carlo simulation involving  $10^6$  samples. Since the exact integral is zero regardless of the dimension  $N$ , both dimension-reduction and Monte Carlo methods can be evaluated. Fig. 2 shows the absolute errors provided by these two methods. For smaller values of  $N$ , the error produced by the Monte Carlo simulation fluctuates slightly about zero and then begins to deviate from zero when  $N > 15$ . In contrast, the proposed dimension-reduction method yields exact results regardless of the value of  $N$ . The superior performance of the dimension-reduction method can be explained by noting that the residual error (see Eq. (12)) is zero, because all even-order derivatives vanish at the expansion point.

**Example 4.** Let

$$I[y(x_1, \dots, x_N)] \equiv \int_0^1 \cdots \int_0^1 \left( \sum_{i=1}^N x_i \right)^{1/2} \prod_{i=1}^N dx_i \quad (48)$$

denote another  $N$ -dimensional integral, for which Entacher [24] developed a quasi-Monte Carlo formula involving a generalized Haar series to determine the integration error. From the reported results in Ref. [24], Table 2 shows

the integration errors by two quasi-Monte Carlo analyses involving 32,768 and 262,144 function evaluations of the integrand. The error measures, which vary from  $4.0 \times 10^{-8}$  to  $3.4 \times 10^{-1}$  for 32,768 evaluations and  $2.1 \times 10^{-10}$  to  $3.4 \times 10^{-1}$  for 262,144 evaluations, strongly depend on the dimension  $N$  and may change by orders of magnitude when  $N$  varies from 6 to 9. When this problem was solved using  $n = 3$  in the univariate dimension-reduction method, only 19–28 function evaluations were required, with integration errors in the order  $10^{-4}$ . The dimension-reduction method is not only computationally efficient, but more importantly, yields error estimates that are relatively insensitive to the dimension of the integral.

**Example 5.** The final example in this set entails calculating standard deviation of the quadratic transformation

$$Y = Y(X_1, \dots, X_N) = \sum_{j=1}^N X_j^2, \quad (49)$$

where  $X_j \mapsto (\mu, \sigma^2)$ ,  $j = 1, \dots, N$  are independent and identically distributed random variables. Recently, Hong [19] proposed a point estimate method to solve this problem for three distinct cases of probability distributions of  $X_j$ : (1) normal, (2) lognormal, and (3) Gamma. Fig. 3 shows the plots of relative error  $\varepsilon \equiv (\hat{\sigma}_Y - \sigma_Y)/\sigma_Y$  as a function of the coefficient of variation  $v \equiv \sigma/\mu$  of  $X_j$ , where  $\sigma_Y$  and  $\hat{\sigma}_Y$

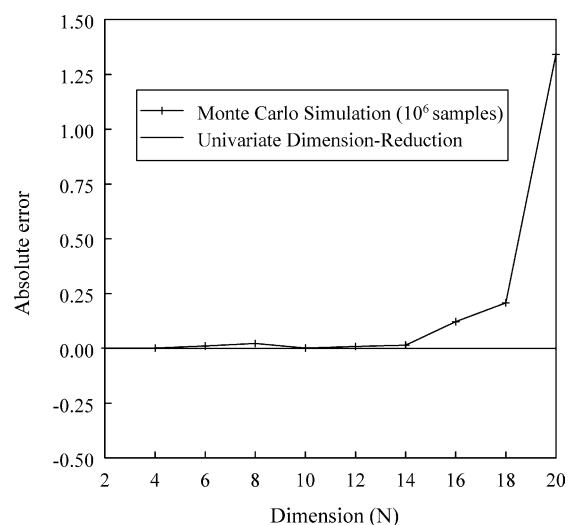


Fig. 2. Absolute errors by univariate dimension-reduction and Monte Carlo methods.

Table 2  
Integration errors by quasi-Monte Carlo and dimension-reduction methods

Dimension (N)	Integration error		
	Quasi Monte Carlo method [24] (32,768 function evaluations)	Quasi Monte Carlo method [24] (262,144 function evaluations)	Univariate dimension-reduction method (19–28 function evaluations) <sup>a</sup>
6	$4.0 \times 10^{-8}$	$2.1 \times 10^{-10}$	$3.6 \times 10^{-4}$
7	$1.5 \times 10^{-5}$	$1.4 \times 10^{-8}$	$2.6 \times 10^{-4}$
8	$1.7 \times 10^{-4}$	$5.9 \times 10^{-6}$	$2.0 \times 10^{-4}$
9	$3.4 \times 10^{-1}$	$3.4 \times 10^{-1}$	$1.6 \times 10^{-4}$

<sup>a</sup> Required 19, 22, 25, and 28 functions evaluations for  $N = 6, 7, 8,$  and  $9,$  respectively.

are exact and approximate standard deviations of  $Y$ , respectively. The relative error by the point estimate method is independent of  $N$ , but its accuracy degrades when the input coefficient of variation  $\nu$  is large [19]. In contrast, the dimension-reduction method, which has a zero residual error (see Eq. (12)), provides exact estimates of the standard deviation of  $Y$  regardless of the dimension of the problem and the coefficient of variation of input.

4.2. Example Set II: solid-mechanics problems

In most of these solid-mechanics examples, random fields are introduced to increase the dimension of the stochastic problem. For example, lognormal random fields were employed in Examples 6 and 9 to represent the spatial variability of material properties. However, in Example 7, the elastic modulus was modeled by a Gaussian random field, which is somewhat unrealistic; but it was adopted here to allow for comparing the proposed method with existing methods that require the Gaussian assumption. The proposed method does not require any specific distribution type of input random variables or fields.

**Example 6 (Stochastic finite-difference analysis (linear-elastic)).** Consider a propped cantilever beam on an elastic foundation with its discrete model, as shown in Fig. 4. Suppose that: (1) span  $L = 120$  in.; (2) nodal spacing  $\Delta = L/4 = 30$  in.; (3) constant beam stiffness  $EI = 6.45 \times 10^8$  lb in.<sup>2</sup>; (4) uniformly distributed load  $S = \exp(Z)$  follows a lognormal distribution with mean  $\mu_S = \exp(\mu_Z + \sigma_Z^2/2) = 1000$  lb/in., variance  $\sigma_S^2 = \mu_S^2 [\exp(\sigma_Z^2) - 1]$ , and coefficient of variation  $\nu_S = \sigma_S/\mu_S$ , where  $\mu_Z = \ln(\mu_S/\sqrt{1 + \nu_S^2})$  and  $\sigma_Z^2 = \ln(1 + \nu_S^2)$ ; and (5) the foundation modulus is a homogeneous lognormal random field  $\xi(x) = \exp[\eta(x)]$  with mean  $\mu_\xi = \exp(\mu_\eta + \sigma_\eta^2/2) = 2000$  lb/in.<sup>2</sup>, variance  $\sigma_\xi^2 = \mu_\xi^2 [\exp(\sigma_\eta^2) - 1]$ , and coefficient of variation  $\nu_\xi = \sigma_\xi/\mu_\xi$ , where  $\eta(x)$  is a stationary Gaussian random field with mean  $\mu_\eta$ , variance  $\sigma_\eta^2$ , and covariance function  $\gamma(u) = \mathcal{E}\{[\eta(x+u) - \mu_\eta] \times [\eta(x) - \mu_\eta]\} = \sigma_\eta^2 \exp(-\delta|u|)$ ,  $\delta \geq 0$ . There is no dependence between the applied load and foundation modulus.

The equilibrium equation for the discrete finite-difference model (Fig. 4(b)), including boundary conditions, is

$$\begin{bmatrix} 7 + \zeta X_1 & -4 & 1 \\ -4 & 6 + \zeta X_2 & -4 \\ 1 & -4 & 5 + \zeta X_3 \end{bmatrix} \begin{Bmatrix} Y_1 \\ Y_2 \\ Y_3 \end{Bmatrix} = \begin{Bmatrix} 1 \\ 1 \\ 1 \end{Bmatrix} \zeta X_4 \quad (50)$$

where  $Y_i = Y(i\Delta)$ ,  $i = 1, 2, 3$  is the displacement response at node  $i$ ,  $\zeta = \Delta^4/EI = 1.26 \times 10^{-3}$  in.<sup>2</sup>/lb;  $X_j = \xi(j\Delta) = \exp[\eta(j\Delta)]$ ,  $j = 1, 2, 3$ ; and  $X_4 = S = \exp(Z)$ . The input lognormal vector  $X = \{X_1, X_2, X_3, X_4\}^T \in \mathfrak{R}^4$  has mean  $\mu = \{\mu_\xi, \mu_\xi, \mu_\xi, \mu_S\}^T$  and covariance matrix

$$\gamma = \begin{bmatrix} \sigma_\xi^2 & \sigma_\xi^2 \rho^*(\Delta) & \sigma_\xi^2 \rho^*(2\Delta) & 0 \\ \sigma_\xi^2 \rho^*(\Delta) & \sigma_\xi^2 & \sigma_\xi^2 \rho^*(\Delta) & 0 \\ \sigma_\xi^2 \rho^*(2\Delta) & \sigma_\xi^2 \rho^*(\Delta) & \sigma_\xi^2 & 0 \\ 0 & 0 & 0 & \sigma_S^2 \end{bmatrix}, \quad (51)$$

where  $\rho^*(u) = [\exp\{\gamma(u)\} - 1][\exp(\sigma_\eta^2) - 1]$ . The objective of this example, which was originally presented by Grigoriu [18], is to determine the second-moment characteristics of the displacement response  $Y = \{Y_1, Y_2, Y_3\}^T \in \mathfrak{R}^3$ .

Table 3 gives approximate mean and covariance of  $Y$  for  $\delta\Delta = 0.1$ , obtained using the Monte Carlo simulation

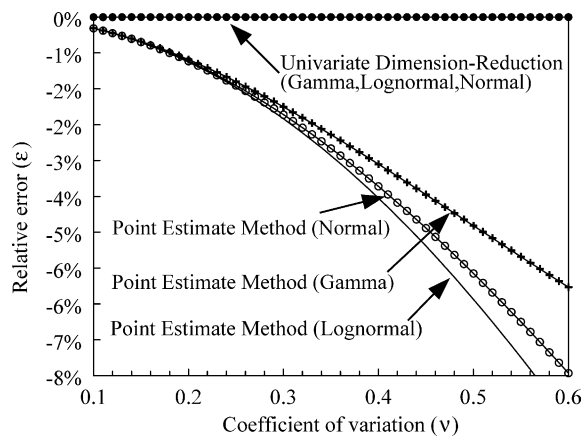


Fig. 3. Relative error  $\varepsilon \equiv (\hat{\sigma}_Y - \sigma_Y)/\sigma_Y$  as a function of input coefficient of variation.

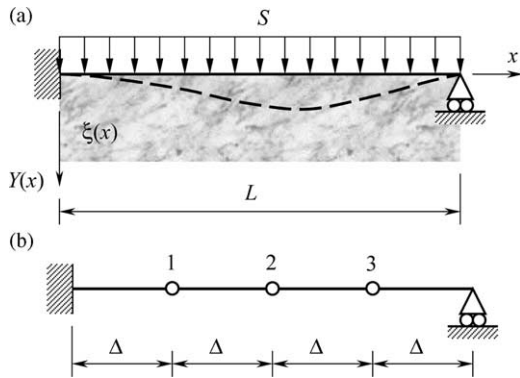


Fig. 4. A stochastic beam on an elastic foundation; (a) geometry and loads; (b) discrete finite-difference model.

(100,000 samples), the univariate dimension-reduction method (Eqs. (40)–(42)), and the statistically equivalent solution [18]. The statistically equivalent solution was developed for stochastic-mechanics problems and was found to be more accurate than first-order Taylor expansion or Neumann expansion methods [18]. The results in Table 3

focus on three cases of input uncertainties: (a)  $\nu_\xi = 0.3$ ,  $\nu_S = 0.2$ ; (b)  $\nu_\xi = 0.6$ ,  $\nu_S = 0.2$ ; and (c)  $\nu_\xi = 0.6$ ,  $\nu_S = 0.01$ . Simulation results and statistically equivalent solutions were obtained from Ref. [18]. In all three cases, the statistically equivalent solution and dimension-reduction method provide almost exact (simulation) estimates of the response mean. However, the dimension-reduction method outperforms the statistically equivalent solution when covariance properties are compared. For example, the ratio of exact to approximate standard deviations lies in the range of (0.81, 1.26) for the statistically equivalent solution and (0.99, 1.04) for the dimension-reduction method. For each stochastic problem, only 13 deterministic analyses ( $n = 3$ ) were required by the dimension-reduction method.

**Example 7 (Stochastic mesh-free analysis (linear-elastic)).** Consider a square plate with a centrally located circular hole, as shown in Fig. 5(a). The plate has

Table 3  
Mean and covariance of displacement vector  $Y$  in beam on elastic foundation for  $\delta\Delta = 0.1$

	Statistically equivalent solution [18]	Univariate dimension-reduction method	Monte Carlo simulation [18] ( $10^6$ samples)
(a) $\nu_\xi = 0.3$ ; $\nu_S = 0.2$			
Mean vector ( $m_Y$ )	$\begin{Bmatrix} 0.295 \\ 0.480 \\ 0.391 \end{Bmatrix}$	$\begin{Bmatrix} 0.297 \\ 0.480 \\ 0.391 \end{Bmatrix}$	$\begin{Bmatrix} 0.297 \\ 0.480 \\ 0.392 \end{Bmatrix}$
Covariance matrix ( $\gamma_Y$ )	$\begin{bmatrix} 0.0044 & 0.0085 & 0.0067 \\ & 0.0168 & 0.0133 \\ \text{(sym.)} & & 0.0107 \end{bmatrix}$	$\begin{bmatrix} 0.0066 & 0.0113 & 0.0091 \\ & 0.0198 & 0.0159 \\ \text{(sym.)} & & 0.0130 \end{bmatrix}$	$\begin{bmatrix} 0.0070 & 0.0121 & 0.0096 \\ & 0.0212 & 0.0170 \\ \text{(sym.)} & & 0.0139 \end{bmatrix}$
(b) $\nu_\xi = 0.6$ ; $\nu_S = 0.2$			
Mean vector ( $m_Y$ )	$\begin{Bmatrix} 0.328 \\ 0.540 \\ 0.441 \end{Bmatrix}$	$\begin{Bmatrix} 0.328 \\ 0.540 \\ 0.439 \end{Bmatrix}$	$\begin{Bmatrix} 0.328 \\ 0.539 \\ 0.439 \end{Bmatrix}$
Covariance matrix ( $\gamma_Y$ )	$\begin{bmatrix} 0.0205 & 0.0388 & 0.0307 \\ & 0.0746 & 0.0595 \\ \text{(sym.)} & & 0.0480 \end{bmatrix}$	$\begin{bmatrix} 0.0163 & 0.0292 & 0.0231 \\ & 0.0535 & 0.0428 \\ \text{(sym.)} & & 0.0348 \end{bmatrix}$	$\begin{bmatrix} 0.0173 & 0.0312 & 0.0247 \\ & 0.0573 & 0.0459 \\ \text{(sym.)} & & 0.0373 \end{bmatrix}$
(c) $\nu_\xi = 0.6$ ; $\nu_S = 0.01$			
Mean vector ( $m_Y$ )	$\begin{Bmatrix} 0.327 \\ 0.540 \\ 0.441 \end{Bmatrix}$	$\begin{Bmatrix} 0.328 \\ 0.540 \\ 0.440 \end{Bmatrix}$	$\begin{Bmatrix} 0.328 \\ 0.540 \\ 0.439 \end{Bmatrix}$
Covariance matrix ( $\gamma_Y$ )	$\begin{bmatrix} 0.0188 & 0.0353 & 0.0279 \\ & 0.0669 & 0.0534 \\ \text{(sym.)} & & 0.0432 \end{bmatrix}$	$\begin{bmatrix} 0.0129 & 0.0238 & 0.0187 \\ & 0.0451 & 0.0360 \\ \text{(sym.)} & & 0.0293 \end{bmatrix}$	$\begin{bmatrix} 0.0126 & 0.0233 & 0.0184 \\ & 0.0442 & 0.0352 \\ \text{(sym.)} & & 0.0285 \end{bmatrix}$

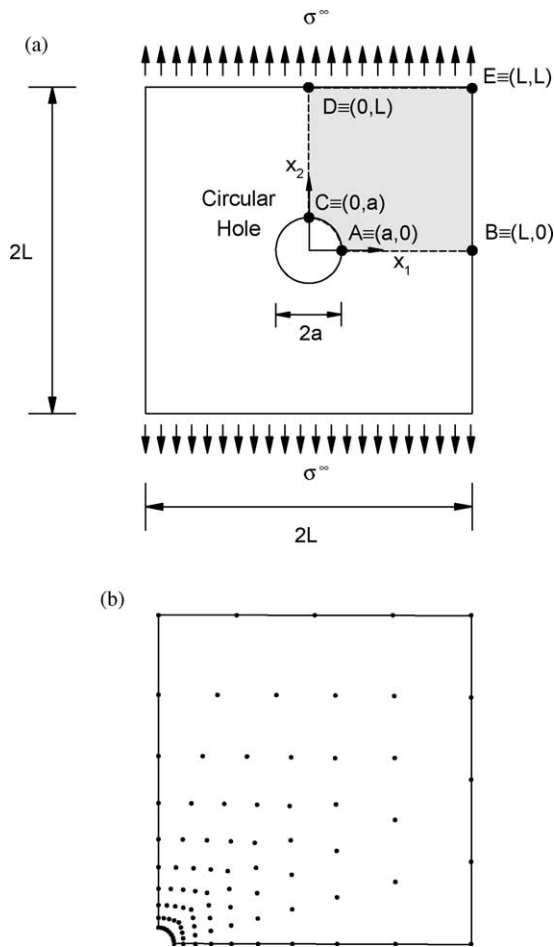


Fig. 5. A square plate with a hole subjected to uniformly distributed tension; (a) geometry and loads; (b) meshless discretization.

a dimension of  $2L = 40$  units, a hole with diameter  $2a = 2$  units, and is subjected to a uniformly distributed load of magnitude  $\sigma^\infty = 1$  unit. The Poisson's ratio  $\nu$  was chosen as 0.3. The elastic modulus was assumed to be a homogeneous random field and symmetrically distributed with respect to  $x_1$ - and  $x_2$ -axes (Fig. 5(a)). The modulus of elasticity  $E(x)$  was represented by  $E(x) = \mu_E[1 + \alpha(x)]$ , where  $\mu_E = 1$  unit is the constant mean over the domain  $\Omega$ , and  $\alpha(x)$  is a homogeneous Gaussian random field with mean zero and covariance function

$$\Gamma_\alpha(\xi) = \mathcal{E}[\alpha(x)\alpha(x + \xi)] = \sigma_\alpha^2 \exp\left[-\frac{\|\xi\|}{bL}\right], \quad \forall x, x + \xi \in \Omega, \quad (52)$$

where  $\sigma_\alpha = 0.1$  unit and  $b = 0.1$  and 0.5. Due to symmetry, only a quarter of the plate, represented by the region ABEDC and shaded in Fig. 5(a), was analyzed. Fig. 5(b) shows a meshless discretization of the quarter plate with 90 nodes [8,15].

The random field  $\alpha(x)$  was parameterized using the Karhunen–Loève expansion [35]

$$\alpha(x) \cong \sum_{j=1}^N X_j \sqrt{\lambda_j} \phi_j(x), \quad (53)$$

where  $X_j \mapsto N(0, 1)$ ,  $j = 1, \dots, N$  are standard and independent Gaussian random variables and  $\{\lambda_j, \phi_j(x)\}$ ,  $j = 1, \dots, N$  are the eigenvalues and eigenfunctions, respectively, of the covariance kernel. The mesh-free shape functions were employed to solve the associated integral equation needed

Table 4a  
Standard deviations of displacement and strains in plate with a hole by various methods ( $b = 0.1$ )

Location	Response variable <sup>a</sup>	Standard deviation of response			
		Second-order Neumann expansion method	Fourth-order Neumann expansion method	Univariate dimension-reduction method	Monte Carlo simulation (5000 samples)
A	$u_1$	$6.45 \times 10^{-2}$	$6.53 \times 10^{-2}$	$6.49 \times 10^{-2}$	$6.54 \times 10^{-2}$
	$\epsilon_{11}$	$1.07 \times 10^{-2}$	$1.08 \times 10^{-2}$	$1.07 \times 10^{-2}$	$1.09 \times 10^{-2}$
	$\epsilon_{22}$	$1.02 \times 10^{-1}$	$1.03 \times 10^{-1}$	$1.02 \times 10^{-1}$	$1.04 \times 10^{-1}$
	$\epsilon_{12}$	$1.46 \times 10^{-2}$	$1.48 \times 10^{-2}$	$1.47 \times 10^{-2}$	$1.49 \times 10^{-2}$
B	$u_1$	$1.96 \times 10^{-1}$	$2.00 \times 10^{-1}$	$1.98 \times 10^{-1}$	$2.00 \times 10^{-1}$
	$\epsilon_{22}$	$4.62 \times 10^{-2}$	$4.67 \times 10^{-2}$	$4.64 \times 10^{-2}$	$4.62 \times 10^{-2}$
C	$u_2$	$1.15 \times 10^{-1}$	$1.16 \times 10^{-1}$	$1.15 \times 10^{-1}$	$1.16 \times 10^{-1}$
	$\epsilon_{11}$	$4.92 \times 10^{-2}$	$4.97 \times 10^{-2}$	$4.94 \times 10^{-2}$	$4.96 \times 10^{-2}$
	$\epsilon_{22}$	$6.23 \times 10^{-3}$	$6.30 \times 10^{-3}$	$6.27 \times 10^{-3}$	$6.26 \times 10^{-3}$
	$\epsilon_{12}$	$2.23 \times 10^{-2}$	$2.26 \times 10^{-2}$	$2.25 \times 10^{-2}$	$2.26 \times 10^{-2}$
D	$u_2$	$4.82 \times 10^{-1}$	$4.98 \times 10^{-1}$	$4.93 \times 10^{-1}$	$5.01 \times 10^{-1}$
	$\epsilon_{22}$	$4.51 \times 10^{-2}$	$4.58 \times 10^{-2}$	$4.55 \times 10^{-2}$	$4.51 \times 10^{-2}$
E	$u_1$	$2.79 \times 10^{-1}$	$2.82 \times 10^{-1}$	$2.81 \times 10^{-1}$	$2.85 \times 10^{-1}$
	$u_2$	$5.34 \times 10^{-1}$	$5.48 \times 10^{-1}$	$5.44 \times 10^{-1}$	$5.59 \times 10^{-1}$
	$\epsilon_{22}$	$4.02 \times 10^{-2}$	$4.08 \times 10^{-2}$	$4.05 \times 10^{-2}$	$4.16 \times 10^{-2}$

<sup>a</sup>  $u_1$  and  $u_2$  are horizontal and vertical displacements, respectively;  $\epsilon_{11}$  and  $\epsilon_{22}$  represent normal tensorial strains in  $x_1$  and  $x_2$  directions, respectively; and  $\epsilon_{12}$  represents tensorial shear strain.

Table 4b  
Standard deviations of displacement and strains in plate with a hole by various methods ( $b = 0.5$ )

Location	Response variable <sup>a</sup>	Standard deviation of response			
		Second-order Neumann expansion method	Fourth-order Neumann expansion method	Univariate dimension-reduction method	Monte Carlo simulation (5000 samples)
A	$u_1$	$1.06 \times 10^{-1}$	$1.11 \times 10^{-1}$	$1.09 \times 10^{-1}$	$1.12 \times 10^{-1}$
	$\varepsilon_{11}$	$2.47 \times 10^{-2}$	$2.58 \times 10^{-2}$	$2.53 \times 10^{-2}$	$2.56 \times 10^{-2}$
	$\varepsilon_{22}$	$2.28 \times 10^{-1}$	$2.39 \times 10^{-1}$	$2.34 \times 10^{-1}$	$2.37 \times 10^{-1}$
	$\varepsilon_{12}$	$3.13 \times 10^{-2}$	$3.28 \times 10^{-2}$	$3.22 \times 10^{-2}$	$3.25 \times 10^{-2}$
B	$u_1$	$4.36 \times 10^{-1}$	$4.60 \times 10^{-1}$	$4.52 \times 10^{-1}$	$4.61 \times 10^{-1}$
	$\varepsilon_{22}$	$7.62 \times 10^{-2}$	$7.97 \times 10^{-2}$	$7.82 \times 10^{-2}$	$8.21 \times 10^{-2}$
C	$u_2$	$2.36 \times 10^{-1}$	$2.48 \times 10^{-1}$	$2.43 \times 10^{-1}$	$2.46 \times 10^{-1}$
	$\varepsilon_{11}$	$8.28 \times 10^{-2}$	$8.64 \times 10^{-2}$	$8.48 \times 10^{-2}$	$8.72 \times 10^{-2}$
	$\varepsilon_{22}$	$1.23 \times 10^{-2}$	$1.28 \times 10^{-2}$	$1.26 \times 10^{-2}$	$1.28 \times 10^{-2}$
	$\varepsilon_{12}$	$3.70 \times 10^{-2}$	$3.89 \times 10^{-2}$	$3.81 \times 10^{-2}$	$3.90 \times 10^{-2}$
D	$u_2$	1.24	1.33	1.30	1.33
	$\varepsilon_{22}$	$7.86 \times 10^{-2}$	$8.30 \times 10^{-2}$	$8.10 \times 10^{-2}$	$8.34 \times 10^{-2}$
E	$u_1$	$5.74 \times 10^{-1}$	$5.94 \times 10^{-1}$	$5.83 \times 10^{-1}$	$5.99 \times 10^{-1}$
	$u_2$	1.30	1.37	1.35	1.38
	$\varepsilon_{22}$	$7.92 \times 10^{-2}$	$8.36 \times 10^{-2}$	$8.17 \times 10^{-2}$	$8.37 \times 10^{-2}$

<sup>a</sup>  $u_1$  and  $u_2$  are horizontal and vertical displacements, respectively.  $\varepsilon_{11}$  and  $\varepsilon_{22}$  represent normal tensorial strains in  $x_1$  and  $x_2$  directions, respectively; and  $\varepsilon_{12}$  represents tensorial shear strain.

to calculate the eigenvalues and eigenfunctions [15]. For the correlation parameter  $b = 0.1$  or  $0.5$ , a value of  $N = 12$  was selected to adequately represent  $\alpha(x)$ . Following the Karhunen–Loève discretization, the input uncertainty is represented by a 12-dimensional standard Gaussian vector  $X \mapsto N(\mathbf{0}, \mathbf{I})$ , where  $\mathbf{0} \in \mathbb{R}^{12}$  and  $\mathbf{I} \in \mathcal{L}(\mathbb{R}^{12} \times \mathbb{R}^{12})$  are the null vector and identity matrix, respectively.

For the correlation parameter  $b = 0.1$  and  $0.5$ , Table 4a and b present standard deviations of displacements and strains at points A, B, C, D, and E (Fig. 5(a)), predicted by the proposed univariate dimension-reduction method (Eqs. (40)–(42)); the second- and fourth-order Neumann expansion methods; and the Monte Carlo simulation (5000 samples). The Neumann expansion solutions were obtained following the development by Ghanem and Spanos [14]. As expected, the fourth-order Neumann expansion method provides more accurate solutions than the second-order version. According to Table 4a and b, the univariate dimension-reduction method also provides satisfactory results of standard deviations when compared with the simulation results. In fact, the accuracy of response statistics from the univariate dimension-reduction method is very close to the accuracy of the fourth-order Neumann expansion method. But the comparison of CPU times, which were obtained for two separate analyses involving  $N = 6$  and  $12$ , and are shown in Fig. 6(a) and (b), respectively, indicates that the dimension-reduction method is far more efficient than both Neumann expansion methods. It would be interesting to pursue multivariate reduction methods, such as the bivariate dimension-reduction method, to determine if it can supersede both the accuracy

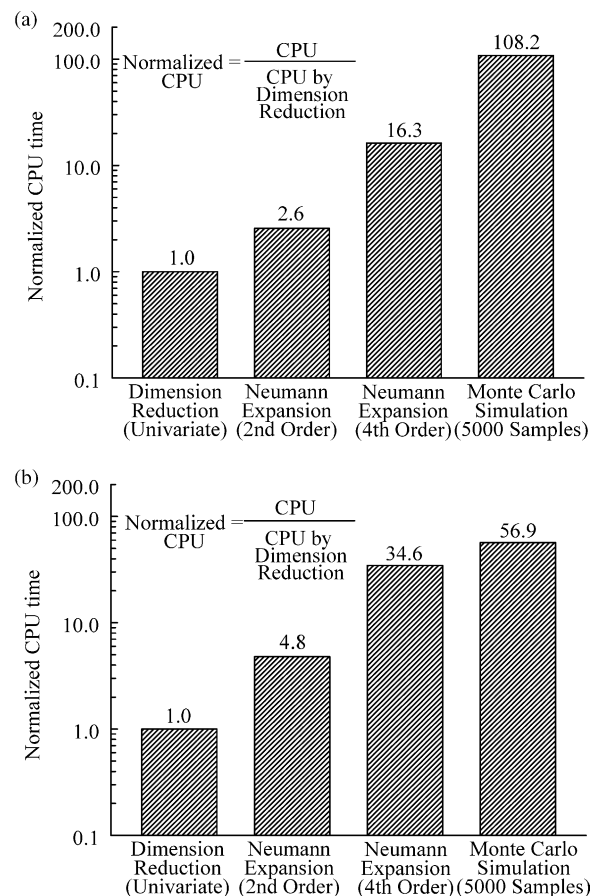


Fig. 6. Comparison of CPU time by various methods; (a)  $N = 6$ ; (b)  $N = 12$ .

and computational efficiency of the fourth-order Neumann expansion method.

**Example 8 (Stochastic finite element analysis (linear-elastic)).** A homogeneous, edge-cracked plate is presented to illustrate a mixed-mode probabilistic fracture-mechanics analysis using the univariate dimension-reduction method. As shown in Fig. 7(a), the plate of length  $L = 16$  units was fixed at the bottom and subjected to a far-field normal stress  $\sigma^\infty$  and a shear stress  $\tau^\infty$  applied at the top. The plate was analyzed by the finite element method including a total of 832 8-noded quadrilateral elements and 48 quarter-point triangular elements at the crack-tip, as shown in Fig. 7(b). The independent random variables involved: (1) uniformly distributed crack length  $a \mapsto U(2.8, 4.2)$  units; (2) uniformly distributed plate width  $W \mapsto U(7, 8)$ ; (3) Gaussian

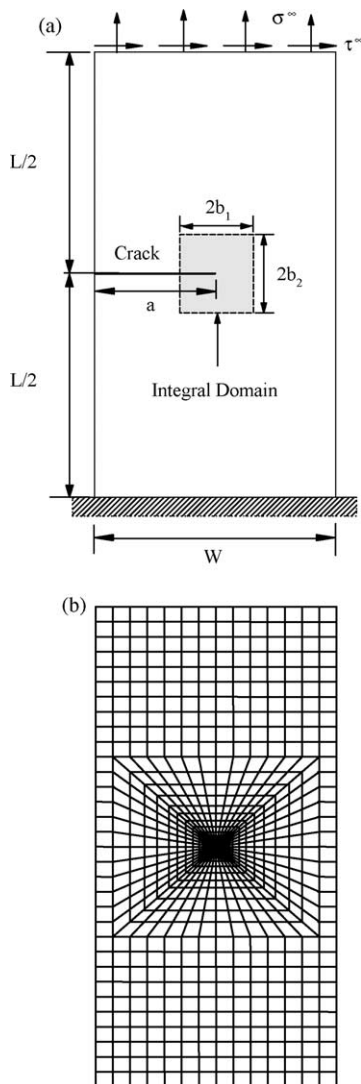


Fig. 7. Edge-cracked plate subject to mixed-mode loading conditions; (a) geometry and loads; (b) finite-element discretization; (c) quarter-point elements at crack tip.

Table 5  
Means and standard deviations of mixed-mode fracture parameters

Response and computational effort	Univariate dimension-reduction method		Monte Carlo simulation	
	Mean	Standard deviation	Mean	Standard deviation
$K_I$	39.302	7.828	39.255	8.033
$K_{II}$	4.411	0.737	4.405	0.739
No. of analyses	13		10,000	

normal stress  $\sigma^\infty \mapsto N(1, 0.1^2)$ ; and (4) Gaussian shear stress  $\tau^\infty \mapsto N(1, 0.1^2)$ . The elastic modulus and Poisson's ratio were  $30 \times 10^6$  units and 0.25, respectively. A plane strain condition was assumed.

Table 5 shows the predicted means and standard deviations of stress-intensity factors  $K_I$  and  $K_{II}$  obtained using the proposed dimension-reduction method (Eq. (24)) and the Monte Carlo simulation (10,000 samples). The results in Table 5 clearly show that the dimension-reduction method can accurately calculate the statistical characteristics of fracture parameters. Only 13 finite element analyses were needed in the dimension-reduction method.

**Example 9 (Stochastic finite element analysis (nonlinear, large-deformation)).** In this example, the proposed dimension-reduction method is employed to solve nonlinear problems in solid-mechanics. Fig. 8(a) shows a shallow circular arch, with mean radius  $R = 100$  mm, rectangular cross-section with depth  $h = 2$  mm, thickness  $t = 1$  mm, and arc angle  $2\beta = 28.1^\circ$ . The arch is fixed at both ends and is subjected to a concentrated load  $P$  at the center. The modulus of elasticity  $E = 80$  kN/mm<sup>2</sup> and Poisson's ratio = 0. A finite element mesh employing 30 8-noded quadrilateral elements is shown in Fig. 8(b). The stress analysis involved large-deformation behavior for modeling the geometric nonlinearity of the arch. A plane stress condition was assumed.

The first effort involved predicting displacement response of the arch when the material properties, geometry, and loads are deterministic. Fig. 9 shows the deflection  $y$  at the central point computed by two methods for loads  $10 \text{ N} \leq P \leq 400 \text{ N}$ . The first method employs the conventional Gauss quadrature rule to construct the element stiffness matrix. For this two-dimensional problem,  $8 \times 8 = 64$  Gauss points were used for each element. The second method uses the proposed dimension-reduction method, where only  $2 \times 8 + 1 = 17$  Gauss points were employed. The displacement responses by both methods are practically identical, but the dimension-reduction method reduces the computational effort of numerical integration by a factor of approximately 4. This computational savings can

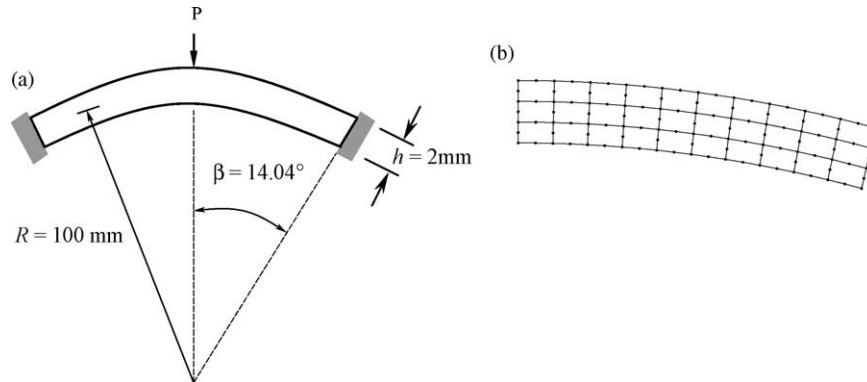


Fig. 8. A shallow arch subject to concentrated load; (a) geometry and loads; (b) finite-element discretization.

become significant in nonlinear stress analysis, since the stiffness matrix must be updated frequently to find an iterative solution to equilibrium equations. However, the reduction factor depends on the order of Gauss quadrature and the spatial dimensions of the problem. Nevertheless, this simple comparison shows how the proposed dimension-reduction method can be exploited for commonly used deterministic analysis.

In the second effort, the modulus of elasticity  $E(x)$  was represented by a homogeneous, lognormal translation field  $E(x) = c_\alpha \exp[\alpha(x)]$ , where mean is  $\mu_E = 80 \text{ kN/mm}^2$ ; standard deviation is  $\sigma_E$ ;  $\alpha(x)$  is a zero-mean, homogeneous, Gaussian random field with standard deviation  $\sigma_\alpha = \sqrt{\ln(1 + \sigma_E^2/\mu_E^2)}$ , an exponential covariance function represented by Eq. (52),  $b = 0.1$ ; and  $c_\alpha = \mu_E \exp(-\sigma_\alpha^2/2) = \mu_E^2 / \sqrt{\mu_E^2 + \sigma_E^2}$ . The Karhunen–Loève expansion was employed to discretize the random field  $\alpha(x)$  into four standard Gaussian random variables.

Due to uncertainty in the elastic modulus, any mechanical response of this arch is stochastic. Table 6 gives estimates of the first five moments  $m_l = E[Y^l]$ ,  $l = 1, \dots, 5$  of the deflection  $Y$  at the central point of the arch, obtained using three approximate methods: (1) the first-order Taylor expansion; (2) the second-order Taylor expansion, and (3) the univariate dimension-reduction method (Eq. (24)). The gradients required in both Taylor expansions were obtained using finite-difference equations. To evaluate approximate methods, direct, four-dimensional numerical integrations were also performed to generate benchmark solutions. The results in Table 6 pertain to four cases of input: (a)  $\sigma_E = 8 \text{ kN/mm}^2$ ,  $P = 400 \text{ N}$ ; (b)  $\sigma_E = 16 \text{ kN/mm}^2$ ,  $P = 400 \text{ N}$ ; (c)  $\sigma_E = 8 \text{ kN/mm}^2$ ,  $P = 200 \text{ N}$ ; and (d)  $\sigma_E = 16 \text{ kN/mm}^2$ ,  $P = 200 \text{ N}$ . The first two cases involve an applied load that yields a mild variation in the deflection. The last two cases entail an applied load that gives rise to instability in the deflection response (Fig. 9). The standard deviation of the elastic modulus was varied for each deflection response. According to the results presented in Table 6, the univariate dimension-reduction method

provides excellent estimates of statistical moments for all four cases of input. For a given problem (case), the proposed method required only  $4 \times 4 + 1 = 17$  analyses ( $n = 4$ ), as opposed to  $4^4 = 256$  analyses using numerical integration. First- and second-order Taylor expansions also yield good estimates of moments, but only for the first two cases of input when the deflection response at the neighborhood of the load ( $P = 400 \text{ N}$ ) is mildly varying and almost linear. However, for the latter two cases ( $P = 200 \text{ N}$ ), deflection behavior is strongly nonlinear, resulting in an unsatisfactory prediction of moments with either Taylor expansion method. In general, the errors are larger for higher-order moments with all three methods. For example, the errors in predicting the first moment (mean) for case (c) by the first-order Taylor expansion, second-order Taylor expansion, and the univariate dimension-reduction method are 5.8, 1.3, and 0.4%, respectively. The respective errors in predicting the fourth moment (kurtosis) for the same case are 32.5, 11.4, and 0.8%, respectively. Nevertheless, the dimension-reduction method provides reasonably good estimates of higher-order moments, and therefore, should provide a better approximation of the tail of response distribution than any Taylor expansion method.

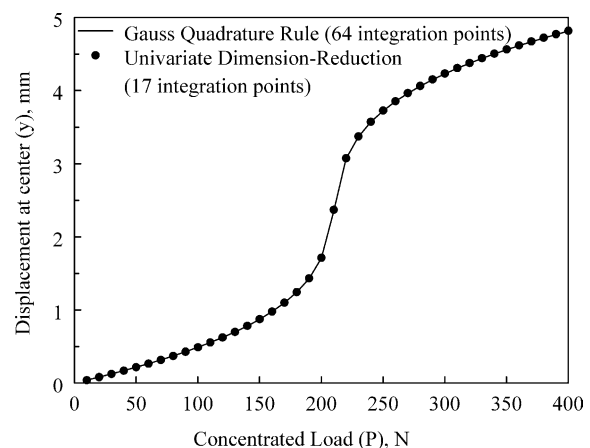


Fig. 9. Deterministic deflection at the center of the arch.

Table 6  
Statistical moments of deflection in shallow arch by various methods

Statistical moments ( $m_i = \mathcal{E}[Y^i]$ )	First-order Taylor expansion method	Second-order Taylor expansion method	Univariate dimension- reduction method	Numerical integration
(a) $\sigma_E = 8 \text{ kN/mm}^2$ ; $P = 400 \text{ N}$				
$m_1$	4.7626	4.7608	4.7609	4.7608
$m_2$	22.689	22.672	22.673	22.672
$m_3$	108.13	108.00	108.01	108.00
$m_4$	515.43	514.65	514.71	514.66
$m_5$	2457.8	2453.1	2453.5	2453.2
(b) $\sigma_E = 16 \text{ kN/mm}^2$ ; $P = 400 \text{ N}$				
$m_1$	4.7892	4.7824	4.7826	4.7823
$m_2$	22.964	22.898	22.900	22.898
$m_3$	110.23	109.76	109.78	109.76
$m_4$	529.78	526.76	526.89	526.79
$m_5$	2549.0	2530.8	2531.7	2531.1
(c) $\sigma_E = 8 \text{ kN/mm}^2$ ; $P = 200 \text{ N}$				
$m_1$	1.6409	1.7192	1.7491	1.7413
$m_2$	2.7641	3.0573	3.1929	3.1735
$m_3$	4.7699	5.6679	6.1191	6.1035
$m_4$	8.4187	11.055	12.382	12.478
$m_5$	15.176	22.908	26.567	27.229
(d) $\sigma_E = 16 \text{ kN/mm}^2$ ; $P = 200 \text{ N}$				
$m_1$	1.7441	2.2288	2.1947	2.0402
$m_2$	3.4769	6.5935	5.3093	4.7406
$m_3$	7.5815	27.000	13.659	12.333
$m_4$	17.761	151.94	36.576	34.904
$m_5$	44.169	1112.7	101.08	104.581

## 5. Conclusions

A new univariate dimension-reduction method was developed for calculating statistical moments of response of mechanical systems subject to uncertainties in loads, material properties, and geometry. This method is based on (1) an additive decomposition of a multi-dimensional response function into multiple one-dimensional functions; (2) an approximation of response moments by moments of single random variables; and (3) a moment-based quadrature rule for numerical integration. The resultant moment equations entail evaluating  $N$  number of one-dimensional integrals, which is substantially simpler and more efficient than performing one  $N$ -dimensional integration. The proposed method does not require the calculation of any partial derivatives of response or the inversion of random matrices, as compared with commonly used Taylor expansion/perturbation methods and Neumann expansion methods, respectively. Hence, the computation effort in conducting stochastic finite element or meshless analyses can be significantly reduced. Two sets of numerical examples, one involving elementary mathematical functions and the other involving solid-mechanics problems, are presented to illustrate the proposed method. The accuracy and computational efficiency of the proposed method were evaluated by simulation or direct numerical integration

and were also compared with alternative analytical methods. The results of five mathematical examples indicate that the univariate dimension-reduction method provides more accurate estimates of statistical moments or multidimensional integration than the first- and second-order Taylor expansion methods, the quasi-Monte Carlo simulation, and the point estimate method. Solid-mechanics examples include both linear and nonlinear problems analyzed by the finite-difference, finite element, and meshless methods. The results of four solid-mechanics examples illustrate that the univariate dimension-reduction method outperforms first- and second-order Taylor expansion methods, the second-order Neumann expansion method, and statistically equivalent solutions. In one example, the accuracy of the univariate dimension-reduction method is comparable in accuracy to the fourth-order Neumann expansion method, but a CPU time comparison suggests that the former method is far more efficient than the latter.

## Acknowledgements

The authors would like to acknowledge the financial support of the US National Science Foundation (Grant Nos CMS-9733058, CMS-9900196 and DMS-0355487) and the US Army sponsored Automotive Research Center.

## References

- [1] Grigoriu M. Stochastic calculus: applications in science and engineering. Basel/New York, NY: Birkhäuser/Springer; 2002.
- [2] Madsen HO, Krenk S, Lind NC. Methods of structural safety. Englewood Cliffs, NJ: Prentice-Hall; 1986.
- [3] IASSAR Subcommittee on Computational Stochastic Structural Mechanics. A state-of-the-art report on computational stochastic mechanics. In: Schueller GI, editor. Probabilistic engineering mechanics, 12.; 1997. p. 197–321.
- [4] Genz AC, Keister BD. Fully symmetric interpolatory rules for multiple integrals over infinite regions with Gaussian weight. J Comput Appl Math 1996;71:299–309.
- [5] Genz AC, Monahan J. A stochastic algorithm for high-dimensional integrals over unbounded regions with Gaussian weight. J Comput Appl Math 1999;112:71–81.
- [6] Genz AC, Malik AA. An imbedded family of fully symmetric numerical integration rules. SIAM J Numer Anal 1983;20.
- [7] Kleiber M, Hien TD. The stochastic finite element method. New York, NY: Wiley; 1992.
- [8] Rahman S, Rao BN. A perturbation method for stochastic meshless analysis in elastostatics. Int J Numer Meth Engng 2001;50:1969–91.
- [9] Liu WK, Belytschko T, Mani A. Random field finite elements. Int J Numer Meth Engng 1986;23:1831–45.
- [10] Shinozuka M, Astill J. Random eigenvalue problems in structural mechanics. AIAA J 1972;10:456–62.
- [11] Adomian G, Malakian K. Inversion of stochastic partial differential operators: the linear case. J Math Anal Appl 1980;77:505–12.
- [12] Yamazaki F, Shinozuka M. Neumann expansion for stochastic finite element analysis. ASCE J Engng Mech 1988;114:1335–54.
- [13] Spanos PD, Ghanem RG. Stochastic finite element expansion for random media. ASCE J Engng Mech 1989;115:1035–53.
- [14] Ghanem RG, Spanos PD. Stochastic finite elements: a spectral approach. New York, NY: Springer; 1991.
- [15] Rahman S, Xu H. A meshless method for computational stochastic mechanics. Int J Comput Engng Sci 2004; in press.
- [16] Adomian G. Applied stochastic processes. New York, NY: Academic Press; 1980.
- [17] Adomian G. Stochastic systems. New York, NY: Academic Press; 1980.
- [18] Grigoriu M. Statistically equivalent solutions of stochastic mechanics problems. ASCE J Engng Mech 1991;117:1906–18.
- [19] Hong HP. An efficient point estimate method for probabilistic analysis. Reliab Engng Syst Safety 1998;59:261–7.
- [20] Rosenblueth E. Two-point estimates in probabilities. Appl Math Modelling 1981;5:329–35.
- [21] Rubinstein RY. Simulation and the Monte Carlo method. New York, NY: Wiley; 1981.
- [22] Niederreiter H, Spanier J. Monte Carlo and quasi-Monte Carlo methods. Berlin: Springer; 2000.
- [23] Sobol IM. On quasi-Monte Carlo integrations. Math Computers Simul 1998;47:103–12.
- [24] Entacher K. Quasi-Monte Carlo methods for numerical integration of multivariate Haar series. BIT3 1997;4:845–60.
- [25] Englund S, Rackwitz R. A benchmark study on importance sampling techniques in structural reliability. Struct Safety 1993;12:255–76.
- [26] Melchers RE. Importance sampling in structural systems. Struct Safety 1989;6:3–10.
- [27] Bjerager P. Probability integration by directional simulation. ASCE J Engng Mech 1988;114:1285–302.
- [28] Nie J, Ellingwood BR. Directional methods for structural reliability analysis. Struct Safety 2000;22:233–49.
- [29] McKay MD, Conover WJ, Beckman RJ. A comparison of three methods for selecting values of input variables in the analysis of output from a computer code. Technometrics 1979;21:239–45.
- [30] Stein M. Large sample properties of simulations using latin hypercube sampling. Technometrics 1987;29:143–50.
- [31] Gilks WR, Richardson S, Spiegelhalter DJ. Markov chain Monte Carlo in practice. London: Chapman-Hall; 1996.
- [32] Nelson BL. Decomposition of some well-known variance reduction techniques. J Stat Comput Simul 1986;23:183–209.
- [33] Rosenblatt M. Remarks on a multivariate transformation. Ann Math Stat 1952;23:470–2.
- [34] Abramowitz M, Stegun IA. Handbook of mathematical functions, 9th ed. New York, NY: Dover; 1972.
- [35] Davenport WB, Root WL. An introduction to the theory of random signals and noise. New York: McGraw-Hill; 1958.

Corrigendum

Corrigendum to “A univariate dimension-reduction method for multi-dimensional integration in stochastic mechanics” [Probabilistic Engineering Mechanics 19 (2004) 393–408]<sup>☆</sup>

S. Rahman <sup>\*</sup>, H. Xu

Department of Mechanical Engineering, College of Engineering, University of Iowa, 2140 Seamans Center, Iowa City, IA 52242, USA

Available online 30 September 2005

In Example 7, the results listed in Tables 4a and 4b of the above article were calculated when the covariance function  $\Gamma_{\alpha}(\xi) = \sigma_{\alpha} \exp[-(|\xi_1| + |\xi_2|)/(bL)]$ ,  $\forall \mathbf{x}, \mathbf{x} + \xi \in \Omega$ .

For the isotropic covariance function described by Eq. (52), the corrected Tables 4a and 4b should read as follows:

The authors apologize for any inconvenience caused.

Table 4a  
Standard deviations of displacement and strains in plate with a hole by various methods ( $b=0.1$ )

Location	Response variable <sup>a</sup>	Standard deviation of response			
		2nd-order Neumann expansion method	4th-order Neumann expansion method	Univariate dimension-reduction method	Monte Carlo simulation (5000 samples)
A	$u_1$	$7.57 \times 10^{-2}$	$7.70 \times 10^{-2}$	$7.63 \times 10^{-2}$	$7.84 \times 10^{-2}$
	$\varepsilon_{11}$	$1.31 \times 10^{-2}$	$1.32 \times 10^{-2}$	$1.31 \times 10^{-2}$	$1.32 \times 10^{-2}$
	$\varepsilon_{22}$	$1.25 \times 10^{-1}$	$1.26 \times 10^{-1}$	$1.26 \times 10^{-1}$	$1.27 \times 10^{-1}$
	$\varepsilon_{12}$	$1.78 \times 10^{-2}$	$1.81 \times 10^{-2}$	$1.79 \times 10^{-2}$	$1.82 \times 10^{-2}$
B	$u_1$	$2.29 \times 10^{-1}$	$2.35 \times 10^{-1}$	$2.32 \times 10^{-1}$	$2.38 \times 10^{-1}$
	$\varepsilon_{22}$	$5.02 \times 10^{-2}$	$5.10 \times 10^{-2}$	$5.06 \times 10^{-2}$	$5.06 \times 10^{-2}$
C	$u_2$	$1.38 \times 10^{-1}$	$1.40 \times 10^{-1}$	$1.39 \times 10^{-1}$	$1.41 \times 10^{-1}$
	$\varepsilon_{11}$	$5.79 \times 10^{-2}$	$5.88 \times 10^{-2}$	$5.83 \times 10^{-2}$	$5.99 \times 10^{-2}$
	$\varepsilon_{22}$	$7.47 \times 10^{-3}$	$7.58 \times 10^{-3}$	$7.53 \times 10^{-3}$	$7.75 \times 10^{-3}$
	$\varepsilon_{12}$	$2.62 \times 10^{-2}$	$2.67 \times 10^{-2}$	$2.65 \times 10^{-2}$	$2.72 \times 10^{-2}$
D	$u_2$	$5.66 \times 10^{-1}$	$5.89 \times 10^{-1}$	$5.83 \times 10^{-1}$	$5.83 \times 10^{-1}$
	$\varepsilon_{22}$	$4.94 \times 10^{-2}$	$5.03 \times 10^{-2}$	$4.98 \times 10^{-2}$	$4.92 \times 10^{-2}$
E	$u_1$	$3.21 \times 10^{-1}$	$3.25 \times 10^{-1}$	$3.23 \times 10^{-1}$	$3.23 \times 10^{-1}$
	$u_2$	$6.20 \times 10^{-1}$	$6.40 \times 10^{-1}$	$6.33 \times 10^{-1}$	$6.35 \times 10^{-1}$
	$\varepsilon_{22}$	$4.77 \times 10^{-2}$	$4.86 \times 10^{-2}$	$4.81 \times 10^{-2}$	$4.76 \times 10^{-2}$

<sup>a</sup>  $u_1$  and  $u_2$  are horizontal and vertical displacements, respectively.  $\varepsilon_{11}$  and  $\varepsilon_{22}$  represent normal tensorial strains in  $x_1$  and  $x_2$  directions, respectively; and  $\varepsilon_{12}$  represents tensorial shear strain.

<sup>☆</sup>DOI of original article: 10.1016/j.probengmech.2004.04.003

<sup>\*</sup> Corresponding author. Tel.: +1 319 335 5679; fax: +1 319 335 5669.

E-mail address: rahman@engineering.uiowa.edu (S. Rahman).

Table 4b  
Standard deviations of displacement and strains in plate with a hole by various methods ( $b=0.5$ )

Location	Response variable <sup>a</sup>	Standard deviation of response			
		2nd-order Neumann expansion method	4th-order Neumann expansion method	Univariate dimension-reduction method	Monte Carlo simulation (5000 samples)
A	$u_1$	$1.11 \times 10^{-1}$	$1.17 \times 10^{-1}$	$1.15 \times 10^{-1}$	$1.19 \times 10^{-1}$
	$\varepsilon_{11}$	$2.64 \times 10^{-2}$	$2.78 \times 10^{-2}$	$2.72 \times 10^{-2}$	$2.79 \times 10^{-2}$
	$\varepsilon_{22}$	$2.44 \times 10^{-1}$	$2.57 \times 10^{-1}$	$2.51 \times 10^{-1}$	$2.58 \times 10^{-1}$
	$\varepsilon_{12}$	$3.34 \times 10^{-2}$	$3.52 \times 10^{-2}$	$3.45 \times 10^{-2}$	$3.54 \times 10^{-2}$
B	$u_1$	$4.63 \times 10^{-1}$	$4.92 \times 10^{-1}$	$4.83 \times 10^{-1}$	$4.95 \times 10^{-1}$
	$\varepsilon_{22}$	$8.18 \times 10^{-2}$	$8.58 \times 10^{-2}$	$8.41 \times 10^{-2}$	$8.49 \times 10^{-2}$
C	$u_2$	$2.50 \times 10^{-1}$	$2.64 \times 10^{-1}$	$2.58 \times 10^{-1}$	$2.66 \times 10^{-1}$
	$\varepsilon_{11}$	$8.68 \times 10^{-2}$	$9.12 \times 10^{-2}$	$8.92 \times 10^{-2}$	$9.28 \times 10^{-2}$
	$\varepsilon_{22}$	$1.32 \times 10^{-2}$	$1.38 \times 10^{-2}$	$1.35 \times 10^{-2}$	$1.41 \times 10^{-2}$
	$\varepsilon_{12}$	$3.83 \times 10^{-2}$	$4.06 \times 10^{-2}$	$3.97 \times 10^{-2}$	$4.13 \times 10^{-2}$
D	$u_2$	1.34	1.44	1.41	1.44
	$\varepsilon_{22}$	$8.26 \times 10^{-2}$	$8.76 \times 10^{-2}$	$8.53 \times 10^{-2}$	$8.52 \times 10^{-2}$
E	$u_1$	$5.79 \times 10^{-1}$	$6.03 \times 10^{-1}$	$5.91 \times 10^{-1}$	$5.98 \times 10^{-1}$
	$u_2$	1.38	1.46	1.44	1.46
	$\varepsilon_{22}$	$8.25 \times 10^{-2}$	$8.74 \times 10^{-2}$	$8.53 \times 10^{-2}$	$8.59 \times 10^{-2}$

<sup>a</sup>  $u_1$  and  $u_2$  are horizontal and vertical displacements, respectively.  $\varepsilon_{11}$  and  $\varepsilon_{22}$  represent normal tensorial strains in  $x_1$  and  $x_2$  directions, respectively; and  $\varepsilon_{12}$  represents tensorial shear strain.